Nuclear Inst. and Methods in Physics Research, A 959 (2020) 163483

Contents lists available at ScienceDirect

Nuclear Inst. and Methods in Physics Research, A

journal homepage: www.elsevier.com/locate/nima

Novel low resistivity glass: MRPC detectors for ultra high rate applications

Z. Liu [a,b,*], R. Beyer [c], J. Dreyer [c], X. Fan [c], R. Greifenhagen [c], D.W. Kim [e], R. Kotte [c], A. Laso Garcia [c], L. Naumann [c], K. Römer [c], D. Stach [c], C. Uribe Estrada [d], M.C.S. Williams [a,e,f], A. Zichichi [a,f,g]

[a] European Centre for Nuclear Research (CERN), Geneva, Switzerland
[b] ICSC World Laboratory, Geneva, Switzerland
[c] Helmholtz-Zentrum Dresden-Rossendorf, Dresden, Germany
[d] Benemerita Universidad Autonoma de Puebla, Mexico
[e] Gangneung-Wonju National University, Gangneung, South Korea
[f] INFN and Dipartimento di Fisica e Astronomia, Universita di Bologna, Italy
[g] Museo Storico della Fisica e Centro Studi e Ricerche E.Fermi, Roma, Italy

ARTICLE INFO

Keywords:
Multigap resistive plate chamber
Low resistivity glass
Rate capability
Efficiency
Time resolution

ABSTRACT

Multigap Resistive Plate Chambers (MRPCs) are often used as time-of-flight (TOF) detectors for high-energy physics and nuclear experiments thanks to their excellent time accuracy. For the Compressed Baryonic Matter (CBM) TOF system, MRPCs are required to work at particle fluxes on the order of 1–10 kHz/cm^2 for the outer region and 10–25 kHz/cm^2 for the central region. Better time resolution will allow particle identification with TOF techniques to be performed at higher momenta. From our previous studies, a time resolution of 25 ps has been obtained with a 20-gap MRPC of 140 μm gap size with enhanced rate capability. By using a new type of commercially available thin low-resistivity glass, further improvement MRPC rate capability is possible. In order to study the rate capability of the 10-gap MRPC built with this new low-resistivity glass, we have performed tests using the continuous electron beam at ELBE. This 10-gap MRPC, with 160 μm gaps, reaches 97% efficiency at 19.2 kV and a time resolution of 36 ps at particle fluxes near 2 kHz/cm^2. At a flux of 100 kHz/cm^2, the efficiency is still above 95% and a time resolution of 50 ps is obtained, which would fulfil the requirement of CBM TOF system.

1. Introduction

The excellent timing performance of Multigap Resistive Plate Chambers (MRPCs) makes them widely used in high energy and nuclear physics experiments [1–3]. The detectors for future experiments require higher rate capabilities as well as timing precision. As an example, the Compressed Baryonic Matter (CBM) experiment is planned to operate at the Facility for Antiproton and Ion Research (FAIR) to study nucleus–nucleus collisions [4]. For the Time of flight (TOF) system of CBM experiment, MRPCs will be required to work at particle fluxes on the order of 1–10 kHz/cm^2 for the outer region and 10–25 kHz/cm^2 for the central region [5]. Thus the rate capability is a key factor for the MRPCs used at the CBM experiment. Better time resolution under high flux will also allow particle identification with TOF techniques to be performed at higher momenta. Thus there is an urgent need for MRPCs which can work at a higher incident flux of particles and operate reliably with a time resolution approaching 20 ps for through-going particles.

Building an MRPC with a time resolution better than 20 ps while maintaining high efficiency is possible, as reported in [6]. Our R&D goal is to design and build an MRPC with similar performance, while operated with a high flux of particles. Additionally we want to maintain the feasibility of building a large area detector, together with low cost, ease of construction, with a minimum material budget. Starting from the design presented in [7], a time resolution of 25 ps has been obtained with 20-gap MRPC with a 140 μm gap size [8].

A fundamental parameter for MRPCs is the rate capability. Lower resistivity materials have been shown to improve the rate capability of MRPCs [9,10]. However, low-resistivity material is often thicker (more than 0.7 mm) than commercial soda-lime float glass (with values down to 0.28 mm). Using thicker plates increases the material budget and thus imposes a practical limit to the number of gas gaps; reducing the number of gas gaps (with increased gap size) makes precise timing more of a challenge. We have obtained new low-resistivity glass samples[1] with 0.4 mm thickness, which are commercially available. It should be noted that this glass is manufactured by industry using standard high

* Corresponding author at: European Centre for Nuclear Research (CERN), Geneva, Switzerland.
E-mail address: zheng.liu@cern.ch (Z. Liu).

[1] The samples were received from Picotech SAS.

https://doi.org/10.1016/j.nima.2020.163483
Received 3 December 2019; Received in revised form 18 January 2020; Accepted 20 January 2020
Available online 21 January 2020

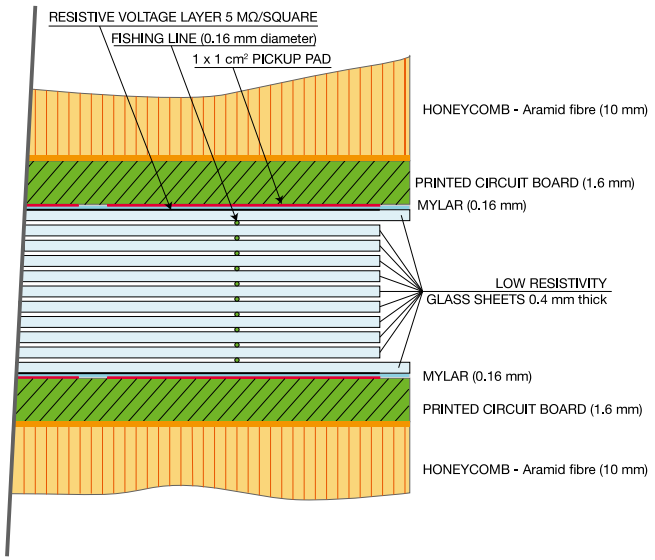

Fig. 1. Cross section view of the 10-gap pad MRPC.

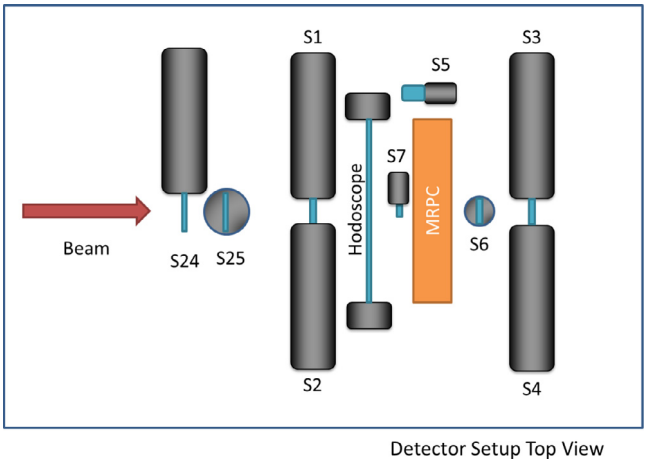

Fig. 2. The experimental setup for MRPC test in the ELBE test beam facility.

volume production techniques. A 6 gap-MRPC with all plates made from this low-resistivity glass was tested in the PS T10 beam facility at CERN [11]. It reached 90% efficiency at an instantaneous flux of 90 kHz/cm^2. However, this test was made with a pulsed beam (spill of 360 ms every 15 s) with the beam just covering a small portion of the active area of the MRPC. As a result, there is the possibility of an overestimation of the rate capability compared with a continuous full area irradiation.

The Electron Linac for beams with high Brilliance and low Emittance (ELBE) [12], at the Helmholtz-Zentrum Dresden-Rossendorf (HZDR) in Germany, produces a continuous tuneable flux electron beam with a beam spot around 3.5 cm diameter; therefore it is an ideal location to test our new MRPC prototype (a 10-gap pad readout MRPC with low-resistivity glass) to measure its rate capability.

2. MRPC construction

A 10-gap MRPC with pad readout (from now on referred to as the pad MRPC) was built for the study. The active area of the pad MRPC is 5 × 6 cm^2. It has a 4 × 4 array of 1 × 1 cm^2 readout pads.

This pad MRPC has a single-stack geometry. The stack is formed as 10 gas gaps with 2 outer glass plates and 9 inner glass plates. This low

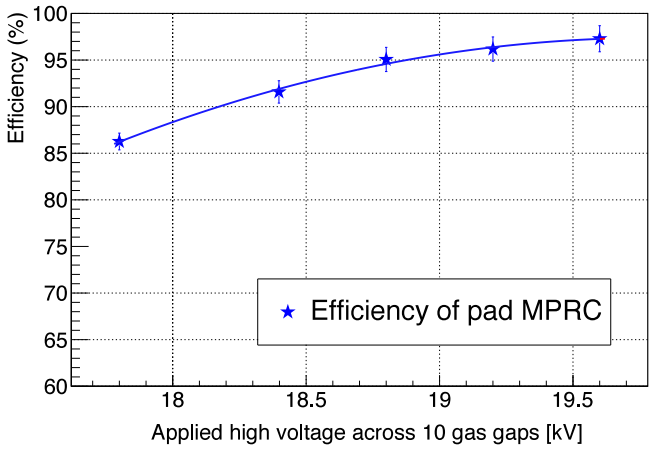

Fig. 3. The efficiency of the MRPC as a function of different voltages at 2 kHz/cm^2. The line through the data points is to guide the eye.

resistivity glass sheet has a bulk resistivity in the order of 10^9 Ω cm and a thickness of 0.4 mm. The outer glass plates of the MRPC has an area of 7 × 9 cm^2 with a 5 × 6 cm^2 voltage electrode; the inner glass plates have an area of 6 × 7 cm^2. The outer surface of the outer glass sheets were painted with resistive material to form a resistive electrode with a surface resistivity of 5 MΩ/□. Fig. 1 shows the cross-section of the MRPC with 10 gas gaps. Fishing line, with a diameter of 160 μm, was used to form a 160 μm gap between the glass plates. A mylar sheet was placed between the resistive electrode and the printed circuit board (PCB) to isolate the high voltage. The MRPC is read out by 10 × 10 mm^2 pads on the top and bottom PCBs. As we have reported previously in [7], reducing the gap size (and increasing the number of gaps) also improves the rate capability of the MRPC with the added advantage of enhancing the timing performance. The MRPC is supported by aramid fibre honeycomb panels and closed inside a gas tight aluminium box.

3. Experimental setup

The MRPC was tested in the electron beam facility at ELBE. A drawing of the experimental setup is shown in Fig. 2. The 30 MeV electron beam had a direction perpendicular to the chamber. The chamber was flushed with a gas mixture of 95% $C_2H_2F_4$ and 5% SF_6. The reference time is given by the RF reference signal and has a time jitter of 35 ps. The two scintillators sets, set 1 (S1, S2) and set 2 (S3, S4) each define an area of 2.0 × 2.0 cm^2. The scintillators of the two sets are read out by photomultiplier tubes (PMTs). All sets are aligned with respect to the beam line and defined a small (2.0 × 2.0 cm^2) area of the beam. By measuring the number of coincidences of the scintillator sets during the spill we can monitor the flux of particles that pass through the MRPC. The MRPC was aligned with the beam line so that the beam was centred in the centre of the active area of the MRPC. The signals from the MRPC are discriminated by the NINO ASIC [13]. The output pulse from the NINO ASIC is sent to an LVDS-to-NIM converter and read out by a WaveCatcher [14] system. The WaveCatcher opens an acquisition window when the trigger from the PMTs' logic signal is valid. The logic signals after the discriminator from the MRPC and time reference PMTs are then sampled and the times of the rising and falling edges are recorded.

In our analysis, if all PMTs register a valid time, this event is regarded as a valid event. If any channel of the MRPC within a certain timing window is recorded with a time-over-threshold (ToT) larger than 8 ns, this is recognised as an MRPC hit. The efficiency of the MRPC is calculated as:

$$\text{Efficiency} = \frac{\text{Total MRPC hits}}{\text{Total valid events}} \quad (1)$$

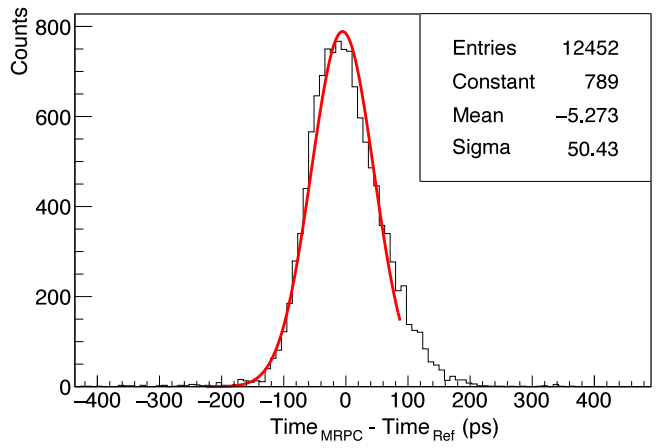

Fig. 4. Time difference between time reference and low-resistivity pad MRPC after slewing corrections. The voltage of the MRPC is 19.2 kV.

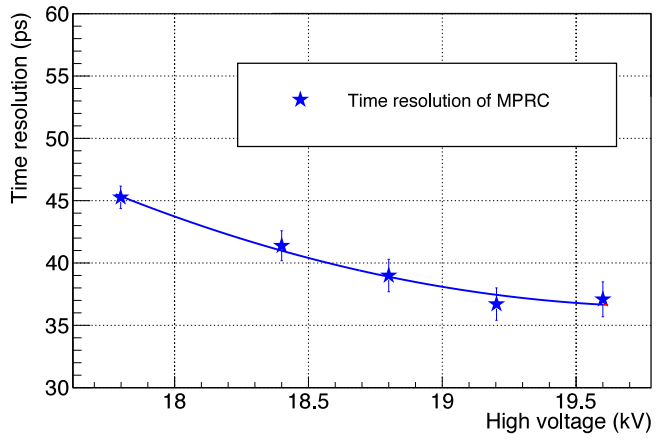

Fig. 5. The time resolution of the MRPC as a function of different voltages at a flux of 2 kHz/cm^2. The line through the data points is to guide the eye.

For the performance study, the MRPC is first tested under different voltages. After the voltage scan, the MRPC is tested at different flux at a set voltage to measure the rate capability.

4. Results

4.1. High voltage scan of MRPC

The MRPC was first tested at a low flux of 2 kHz/cm^2. The efficiency of the MRPC at different voltages is shown in Fig. 3. The maximum efficiency of the MRPC is around 97.0% when the voltage is higher than 19.2 kV. The dark current of the total active area of the 10 gas gap MRPC is below 40 nA when the high voltage is below 19.2 kV.

There will be time slewing dependencies on the input signal amplitude since the NINO chip is set at a fixed threshold for MRPC signal discrimination. A slewing correction needs to be applied based on the time-over-threshold measurement (i.e. the pulse width). Details of the slewing correction procedure can be found in [7]. An example of the time difference between the 10-gap MRPC and the time reference after time-slewing corrections is shown in Fig. 4.

The time resolution of the pad MRPC can be calculated as $\sqrt{50.4^2 - 35^2} = 36$ ps. Following this time-slewing correction technique, we obtained the time resolution of the MRPC at different voltages, which are shown in Fig. 5. The time resolution of the MRPC varies with applied voltages. As the voltage increased from 17.8 kV to 19.6 kV the time resolution of the pad MRPC improved. As can be seen in the figure, the time resolution of the pad MRPC is below 40 ps from 18.5 kV to 19.6 kV. An important measurement is the variation of the absolute time of the signal as a function of the applied voltage. This is shown in Fig. 6.

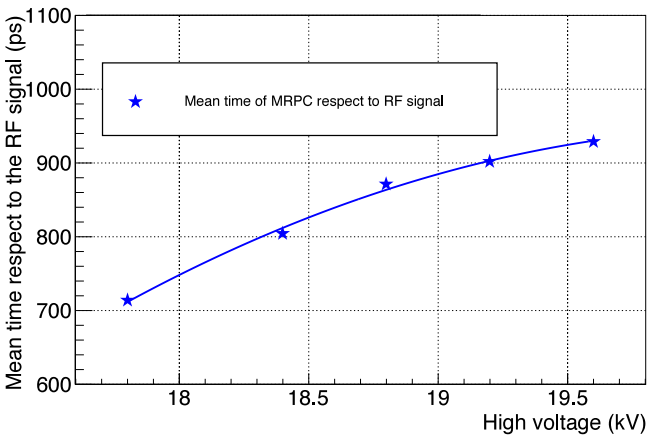

Fig. 6. Reference time minus the time of the MRPC signal for various applied voltages. The error bars are contained within the size of the symbols. The line through the data points is to guide the eye.

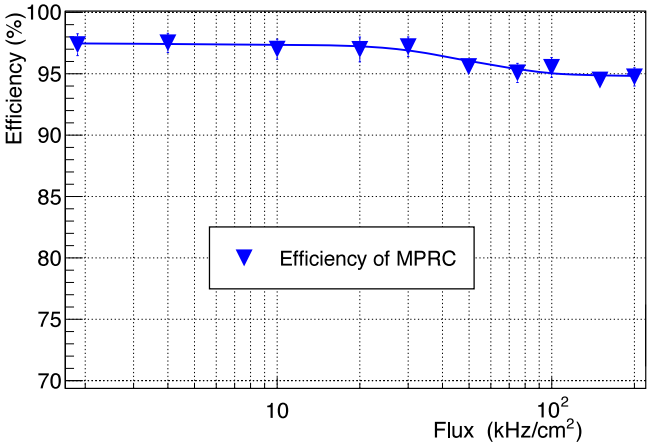

Fig. 7. The efficiency of the MRPC as a function of the flux. The flux is measured with the scintillators S1S2. The high voltage of the 10-gap MRPC is fixed at 19.6 kV. The line through the data points is to guide the eye.

4.2. Flux scan of the MRPC

To test the rate capability of the MRPC, the flux of particles is tuned between 2 kHz/cm^2 and 200.0 kHz/cm^2. The high voltage of the 10-gap MRPC is fixed at 19.6 kV. The efficiency of the MRPC at different fluxes is shown in Fig. 7.

Fig. 8 illustrates the time resolution of the MRPC at different fluxes. The time resolution of the MRPC deteriorates at higher flux. Its time resolution degrades from 37 ps to 60 ps from 2 kHz/cm^2 to 200 kHz/cm^2. The absolute time of the MRPC signal with respect to the RF reference signal obtained during the scan of the flux of the electron beam is shown in Fig. 9. We can use these measurements to infer the voltage drop on the glass plates by using Fig. 6.

5. Resistivity of the glass

In our previous report [11], we quoted a resistivity value of this glass as 2.1 × 10^{10} Ω cm at 24 °C. This value is measured with a

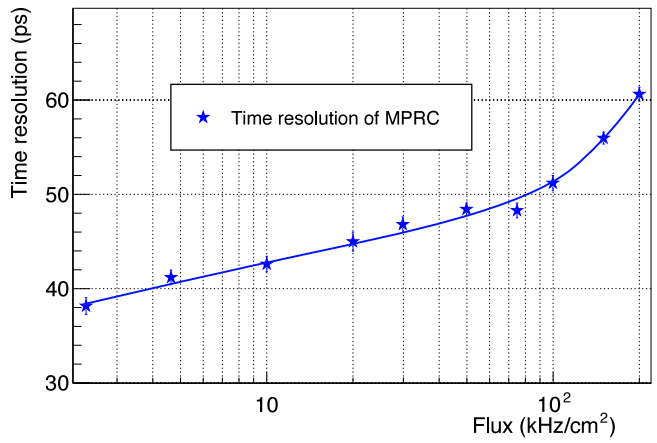

Fig. 8. The time resolution of the MRPC as a function of the flux. The flux is measured with the scintillators S1S2. The high voltage of the 10-gap MRPC is fixed at 19.6 kV. The line through the data points is to guide the eye.

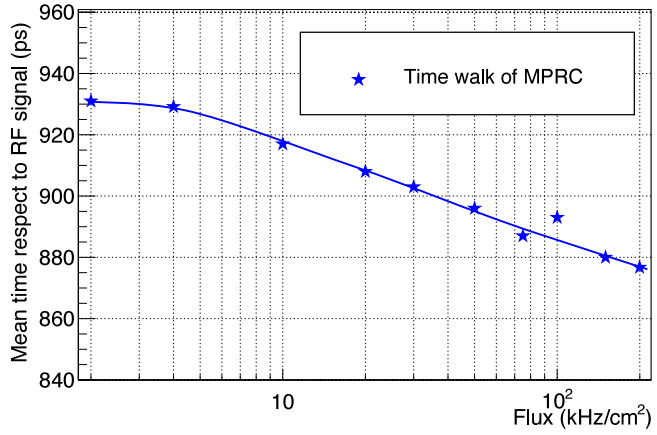

Fig. 9. The absolute time of the MRPC signal with respect to the RF reference signal. The flux is measured with the scintillators S1S2. The error bars are contained within the size of the symbol. The line through the data points is to guide the eye.

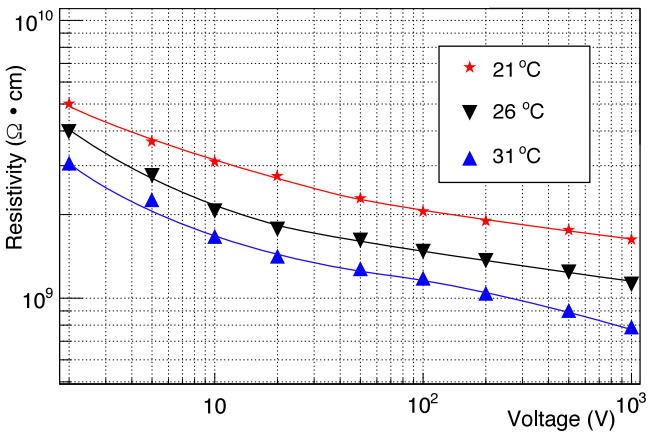

Fig. 10. The bulk resistivity decreases as the voltage is increased across the piece of 0.4 mm glass under test. Each resistivity point is measured after applying the voltage for two minutes.

resistance meter with one day stability. However, we found that the resistivity of glass varies both with applied voltage (see Fig. 12) and the accumulated charge passed through it. Fig. 11 shows the resistivity versus the accumulated charge after passing current through a sample of glass. Three measurements corresponding to different applied voltages are shown. The resistivity starts at $\sim 10^9$ Ω cm and rises to 10^{11} Ω cm. It is probable that the resistivity would continue to rise if we continued to pass current through the glass sheet. There are some notable aspects observable in this plot: (a) the resistivity has a lower value when the applied voltage is higher (the variation of resistivity versus voltage is shown in Fig. 10); (b) the increase in resistivity happens at lower accumulated charge for lower applied voltage (although it actually takes a longer time). If the electric field in the glass is reversed, the resistivity starts to decrease as shown in Fig. 12. In this case the resistivity decreases to a value of 7.5×10^9 Ω cm; a value higher than the initial value. The resistivity change under reversed electric field in a long time measurement is shown in Fig. 13. The electric field has been reversed three times and the trend is an increase of resistivity. So an optimised electric field polarity change point to get the best performance will be important and is under study.

6. Discussion

Charged particles passing through an MRPC create gas avalanches. The movement of the electrons generates the fast signal (which is the usual observed signal); however there is the slow signal generated by the movement of predominantly positive ions drifting towards the cathode. When the gas gap is small, the avalanche process is strongly modified by space charge [15,16]. For a 10 gap MRPC with a gap size of 160 μm, we expect the total charge produced by each through-going particle to be 1.2 pC. At ELBE the beam spot has a 3.5 cm diameter, i.e. a beam spot of 10 cm^2. The current drawn by the MRPC at 100 kHz/cm^2 is 1.2 μA and this matches the expected total charge generated in the MRPC for each through-going charged particle. We have introduced a way to estimate the voltage drop at high flux in [11]. The formation of the avalanche become earlier in time with stronger electric field at higher voltage, so there will be a time shift as a function of applied voltage. From the comparison of the time shift at different voltage and the time information at different flux we can estimate the voltage drop at different flux. From Figs. 6 and 9 we can deduce that the voltage drop is ~500 V. This voltage drop information and current drawn allows us to calculate the resistivity of the glass to be 9.5×10^9 Ω cm. From Fig. 11, we see that this requires a charge of 10 mC to be passed through the glass. Running continuously at a rate of 100 kHz/cm^2 for 24 h would generate such an accumulated charge. However, based on our calculation, the total charge passed through the glass was 4.35 mC when the MRPC was tested at 100 kHz/cm^2, thus the expected resistivity would have been around 5×10^9 Ω cm. This is two times lower than we observed from the time shift method. There could be other effects such as a time shift due to gas pollution at high rate. This will be investigated during a subsequent beam period that we have requested.

One may also consider a rate of 10 kHz/cm^2. Of course the current will be reduced by a factor 10 and a resistivity of 9.5×10^9 Ω cm would result in a voltage drop of 50 V rather than the 500 V observed for 100 kHz/cm^2.

It should be noted that the low resistivity glass used in these tests is not the only glass that shows this behaviour of increasing resistivity with charge transported through the resistive plate. Both ‘soda-lime’ float glass and the low resistivity glass from Tsinghua University exhibit increases in resistivity but may be able to withstand a higher accumulated charge (perhaps ~×10 higher) before this effect becomes significant [17].

Another question relates to the degradation of the time resolution with increasing rate. Part of this may be due to just the higher counting rate introducing noise into the electronics; however we believe that the cause is due to fluctuations with the rate of particles causing a variation in the absolute time as shown in Fig. 9.

The MRPC is a symmetric device; the electric field can be reversed just by reversing the applied voltage. The signals would also reverse in

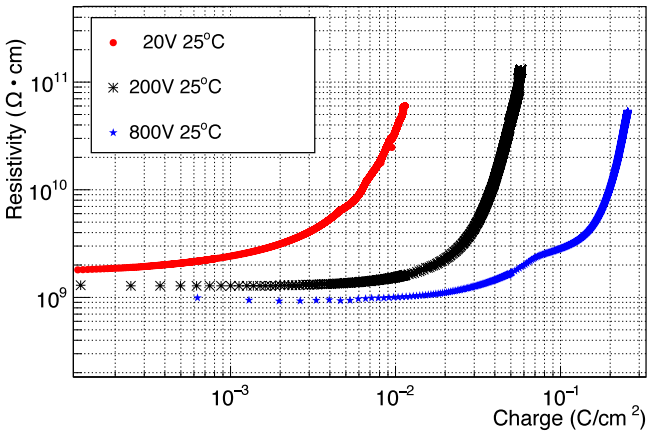

Fig. 11. An increase in resistivity is observed after applying a fixed voltage across a piece of 0.4 mm thick glass.

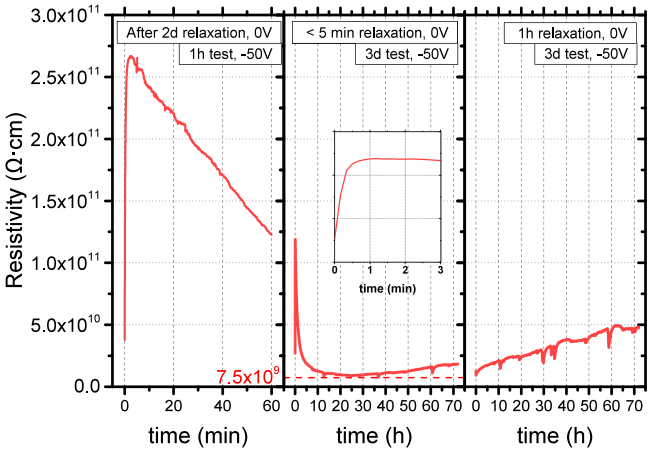

Fig. 12. If the electric field is reversed, the resistivity decreases, but does not return to the initial value.

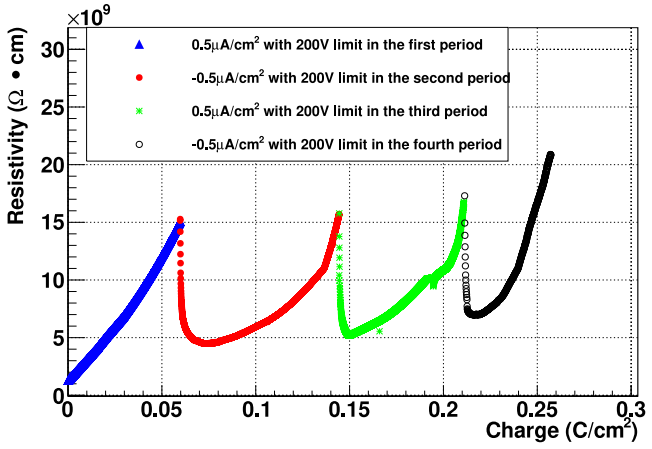

Fig. 13. Long term performance of the glass by reversing the electric field.

polarity thus the front-end electronics need to allow for such a change of polarity. In an environment of a continuous 10 kHz/cm^2 flux, the electric field should be reversed every month to keep the resistivity at a low value.

It should be noted that soda-lime glass plates have a resistivity of 2 to 5 $\times$ 10^{12} Ω cm; thus a flux of 1 kHz/cm^2 would generate a voltage drop on the resistive plates of 1000–2500 V assuming that the avalanches produced by a through-going particle generates a total charge of 1.5 pC. Even if such a 'soda-lime' glass MRPC could maintain a high efficiency, the time shift shown in Fig. 6 (100 ps shift for a change of 1000 V) would significantly degrade the time resolution.

Declaration of competing interest

The authors declare that they have no known competing financial interests or personal relationships that could have appeared to influence the work reported in this paper.

CRediT authorship contribution statement

Z. Liu: Project administration, Writing - original draft, Writing - review & editing, Investigation. **R. Beyer:** Investigation. **J. Dreyer:** Investigation. **X. Fan:** Formal analysis, Investigation, Visualization. **R. Greifenhagen:** Investigation. **D.W. Kim:** Funding acquisition, Writing - review & editing. **R. Kotte:** Investigation. **A. Laso Garcia:** Investigation. **L. Naumann:** Supervision, Writing - review & editing, Investigation, Resources. **K. Römer:** Investigation. **D. Stach:** Investigation. **C. Uribe Estrada:** Funding acquisition, Writing - review & editing, Investigation. **M.C.S. Williams:** Supervision, Writing - original draft, Writing - review & editing. **A. Zichichi:** Funding acquisition, Supervision.

Acknowledgements

Parts of this research were carried out at ELBE at the Helmholtz-Zentrum Dresden — Rossendorf e. V., a member of the Helmholtz Association. We would like to thank for assistance. This work has been supported by the National Research Foundation of Korea, Grant Agreements 2019R1I1A3A01056616, 2019K1A3A1A25000088, the 2019 Academic Research Support Program of Gangneung-Wonju National University, South Korea and project No. A1-S-39980, CB-2017-2018 jointly sponsored by SEP and CONACYT, Mexico.

References

[1] A.N. Akindinov, et al., Latest results on the performance of the multigap resistive plate chamber used for the ALICE TOF, Nucl. Instrum. Methods Phys. Res. A 533 (1) (2004) 74–78.
[2] D. Belver, et al., The HADES RPC inner TOF wall, Nucl. Instrum. Methods Phys. Res. A 602 (2009) 687–690.
[3] B. Bonner, et al., A multigap resistive plate chamber prototype for time- of-flight for the STAR experiment at RHIC, Nucl. Instrum. Methods Phys. Res. A 478 (2002) 176–179.
[4] Johann M. Heuser, The compressed baryonic matter experiment at FAIR, in: EPJ Web of Conferences. 13, EDP Sciences, 2011.
[5] I. Deppner, et al., The CBM time-of-flight wall: a conceptual design, J. Instrum. 9 (10) (2014) C10014.
[6] S. An, et al., A 20 ps timing device - A Multigap Resistive Plate Chamber with 24 gas gaps, Nucl. Instrum. Methods Phys. Res. A 594 (1) (2008) 39–43.
[7] Z. Liu, et al., 20 gas gaps multigap resistive plate chamber: Improved rate capability with excellent time resolution, Nucl. Instrum. Methods Phys. Res. A 908 (2018) 383–387.
[8] Z. Liu, et al., Timing performance study of multigap resistive plate chamber with different gap size, Nucl. Instrum. Methods Phys. Res. A 594 (1) (2008) 39–43.
[9] Jingbo Wang, et al., Development of multi-gap resistive plate chambers with low-resistive silicate glass electrodes for operation at high particle fluxes and large transported charges, Nucl. Instrum. Methods Phys. Res. A 621 (1–3) (2010) 151–156.
[10] A. Laso Garcia, et al., Extreme high-rate capable timing resistive plate chambers with ceramic electrodes, J. Instrum. 7 (10) (2012) P10012.
[11] Z. Liu, et al., A multigap resistive plate chamber built with thin low-resistive glass: High rate capability with excellent time resolution, Nucl. Instrum. Methods Phys. Res. A 928 (2019) 7–12.
[12] https://www.hzdr.de.

[13] F. Anghinolfi, et al., NINO: an ultra-fast and low-power front-end amplifier/discriminator ASIC designed for the multigap resistive plate chamber, Nucl. Instrum. Methods Phys. Res. A 533 (1) (2004) 183–187.
[14] D. Breton, J. Maalmi, E. Delagnes, Using Ultra Fast Analog Memories for Fast Photo-detector Read Out, NDIP 2011, Lyon.
[15] C. Lippmann, W. Riegler, Space charge effects in resistive plate chambers, Nucl. Instrum. Methods Phys. Res. A 517 (2004) 54–78.
[16] K. Doroud, H. Afarideh, D. Hatzifotiadou, J. Rahighi, M.C.S. Williams, A. Zichichi, Recombination: An important effect in multigap resistive plate chambers, Nucl. Instrum. Methods Phys. Res. A 610 (2009) 649–653.
[17] M. Morales, C. Pecharromán, G. Mata-Osoro, L.A. Diaz, J.a. Garzón, Ageing and conductivity of electrodes of high rate RPCs from an ion conductivity approach, in: Conference: XI Workshop on Resistive Plate Chambers and Related Detectors, 2012, http://dx.doi.org/10.22323/1.159.0024.